

Beyond the Alphabet: Deep Signal Embedding for Enhanced DNA Clustering

Hadas Abraham¹, Barak Gahtan¹, Adir Kobovich² and Orian Leitersdorf² and Alex M. Bronstein¹ and Eitan Yaakobi¹

¹The Henry & Marilyn Taub Faculty of Computer Science, Technion, Israel

²The Andrew and Erna Viterbi Faculty of Electrical and Computer Engineering, Technion, Israel
 {hadasabraham, barakgahtan, bron, yaakobi}@cs.technion.ac.il,
 {adir.k, orianl}@campus.technion.ac.il

Abstract

The exponential growth of digital data has fueled interest in DNA as a storage medium due to its unmatched density and durability. However, clustering the billions of reads required for error correction and data reconstruction remains a major bottleneck, as traditional edit-distance-based methods are both computationally expensive and prone to data loss. This paper introduces a novel *signal-model* that processes raw Nanopore signals, bypassing the error-prone basecalling step. By directly leveraging analog signal information, the *signal-model* reduces computation time by up to three orders of magnitude compared to edit-distance approaches, while delivering superior accuracy. It also outperforms DNA sequence embedding methods in both accuracy and efficiency. Furthermore, our experiments show that the *signal-model* achieves higher clustering accuracy than existing strand-based algorithms, saving days of computation without compromising quality. Overall, this work represents a significant breakthrough in DNA data storage, highlighting how signal-based analysis can drastically improve both accuracy and scalability.

1 Introduction

Current storage technologies, such as magnetic disks and solid-state drives, are nearing their physical and scalability limits [7], prompting the exploration of alternative solutions [8, 32]. DNA has emerged as a promising alternative storage medium due to its exceptional density—[6, 10, 13, 37] capable of storing exabytes of data per gram—and remarkable durability, enabling data preservation for thousands of years under optimal conditions. A DNA storage pipeline typically comprises four stages: (i) *encoding*, where binary data files are encoded into DNA strands (design files) using error-correcting codes (ECC) [19]; (ii) *synthesis*, which produces artificial DNA strands for each design strand, subsequently stored in a *storage container* [22]; (iii) *sequencing*, where the stored DNA strands are translated back into noisy sequences known as “reads” [1, 10, 27, 37]; and (iv) *retrieval*, where clustering and reconstruction algorithms process the reads, decoding them back into binary data files while correcting errors using

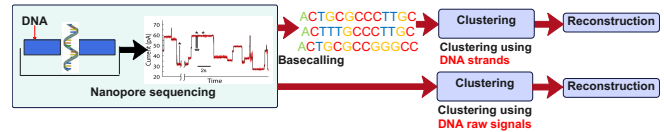


Figure 1: Comparison of traditional DNA clustering pipelines and the proposed approach. The traditional method involves Nanopore sequencing followed by basecalling to generate discrete DNA reads. In contrast, our approach bypasses the basecalling step by directly clustering raw Nanopore signals, reducing errors and computational time.

the selected coding methods. Among these stages, retrieval is particularly challenging due to the vast data scale and the sequencing errors introduced by current technologies.

Nanopore sequencing, the primary DNA sequencer used for DNA storage, enables real-time sequencing of DNA strands. The process involves a single DNA strand passing through a nanopore, causing variations in the measured ionic current. At any given time, the current primarily depends on a nucleotide subsequence of length 4–6 (i.e., a 6-mer) inside the pore. This raw current signal is sampled, resulting in a signal characteristic of the sequence [24, 25].

The signals are then processed by a *basecaller*, which employs deep neural networks to translate the raw signals into nucleotide sequences composed of the bases A, T, C, G [25]. This translation is performed based on the most likely base sequence that could have induced the observed raw signals.

While Nanopore sequencing offers significantly lower costs and enhanced portability compared to traditional Illumina sequencing [15, 20], it also presents several challenges: (1) higher sequencing error rates—approximately 10% of bases suffer from edit, insertion, or deletion errors, compared to only 1% in Illumina [8]; and (2) errors during the signal-to-read translation by the basecaller, which can exclude valid reads, reducing both accuracy and efficiency in downstream clustering and reconstruction tasks. Moreover, the sequencing and basecalling processes can take more than a week in some cases.

Clustering in this context has been explored solely for discrete DNA reads and involves clustering billions of strings¹.

¹The number of clusters in DNA data storage typically ranges

Most DNA clustering algorithms rely on the **edit distance** metric to identify groups of reads likely duplicated from the same source DNA strand. The edit distance between two strings x and y , denoted as $d_e(x, y)$, is defined as the minimum number of edits, deletions, or insertions required to transform x into y [31]. The core challenge of clustering DNA strands in DNA storage lies in the computation of a distance matrix based on the edit distance [21]. This computation has a prohibitive quadratic complexity with respect to both the number and length of the reads, making it unscalable for typical DNA storage datasets, which are extremely large.

Our work addresses challenges in both Nanopore sequencing and clustering for DNA storage by proposing a paradigm shift: directly leveraging raw DNA signals for clustering, thereby bypassing the error-prone basecalling step (see Figure 1). Instead of searching for similarity in discrete DNA reads, our approach operates directly on raw analog DNA signals, which inherently contain richer contextual information. This enables more accurate clustering while minimizing information loss. Specifically, we replace computationally expensive edit-distance calculations with a deep neural network that learns an effective representation of DNA signals by embedding them into a similarity-preserving space. This significantly enhances both scalability and accuracy. We conduct extensive experiments on specialized datasets to demonstrate the effectiveness of our solution and its superior performance compared to DNA strand edit distance.

The key contributions of this work are as follows:

- We introduce a novel framework for directly clustering raw DNA signals during the retrieval stage, eliminating the need for extensive basecalling.
- We develop a deep neural network that generates robust signal embeddings, ensuring high intra-cluster compactness and inter-cluster separability. This approach reduces sample exclusion and minimizes information loss.
- We validate our approach on diverse datasets, achieving up to three orders of magnitude faster computation times compared to traditional methods, while maintaining clustering quality for accurate data reconstruction.

The remainder of this paper is organized as follows. Section 2 reviews related work. Section 3 details the proposed methodology, including both data processing and model design. Next, Section 4 discusses our experimental setup and presents a thorough evaluation of results. Finally, Section 5 concludes the paper.

2 Related Work

Direct utilization of raw signals in DNA storage is challenging. To the best of our knowledge, no existing DNA storage approach directly exploits raw signal data for clustering, reconstruction, or error correction during the retrieval stage. Most prior clustering algorithms operate in the discrete domain and commonly employ edit-distance to compare DNA reads. This introduces high computational overhead rising from two factors: (i) $\mathcal{O}(n^2)$ pairwise comparisons for n reads,

between 1,000 and 100,000, with each cluster containing between 10 and 1,000 samples.

Exp.	No. Clusters	Strand Length	Avg Cluster Size	Avg Strand Length post Basecalling	Creation Time [days]
Microsoft Exp.	10,000	110	300	211	18
Deep DNA Test	110,000	140	10	243	30
Deep DNA Pilot	1,000	140	1,300	240	6

Table 1: Overview of experimental datasets and their key characteristics. The table shows the number of clusters, original strand length (in nucleotides), average cluster size (number of sequences per cluster), average strand length after basecalling, and dataset creation time in days.

and (ii) $\mathcal{O}(\ell^2)$ per-comparison complexity, where ℓ is the read length. Standard dynamic programming implementations of edit-distance [14, 21] are prohibitively expensive at large scales, prompting various mitigation strategies. First, some methods limit the edit-distance depth [3]. Second, others rely on fixed-sized short sub-strings (e.g., Starcode [39]), and still others adopt heuristic-based similarity instead of exact edit-distance (e.g., Clover [28]).

DNA clustering algorithms such as UCLUST [22], CD-HIT [12], and USEARCH [35] combine filtering and approximation strategies to reduce both the number of comparisons and the cost of each comparison. Filtering techniques include hashing approaches like Location Sensitive Hashing (LSH) [2, 5, 30], which group similar strands before performing explicit edit-distance computations. Although these clustering algorithms alleviate some computational bottlenecks, they still face scalability and accuracy trade-offs.

Moving to the signal domain, Dynamic Time Warping (DTW) [34] is the time-series analogue of edit-distance, allowing insertions, deletions, and substitutions for sequences of different lengths. While DTW improves alignment flexibility, its base-case complexity is also quadratic. Despite further optimizations (e.g., limiting the warping window [29]), DTW remains impractical for many-to-many signal comparisons at a typical DNA storage datasets scale. Given that signals can be an order of magnitude longer than discrete DNA strands, DTW-based clustering suffers severely in performance.

A parallel line of work on DNA strand embeddings [11, 16, 23] focuses on learning representations aligned with biological structures (e.g., proteins or genes). However, these embedding methods are task-specific and do not directly apply to synthetic DNA data storage, where the central goal is to recover the original data rather than to capture biological structures.

3 Methodology

This section outlines the proposed framework for clustering raw DNA signals, focusing on the dataset creation, model architecture, and the integration of the ArcFace loss function to ensure robust and scalable embeddings.

Dataset Construction

Public DNA storage datasets do not include raw signals, necessitating the creation of custom datasets that map raw signals to their corresponding DNA reads. To achieve this, experiments encompassing the four stages described in Section 1 were conducted. These stages include *encoding*, where error-correcting

codes were applied to generate design files; *synthesis*, using Twist Bioscience to produce DNA strands; *sequencing*, performed with a Nanopore sequencer over approximately 72 hours; and *basecalling*, translating raw signals into DNA reads, taking about one week. The final step involved creating the signal-strand datasets by calculating the edit distance between each DNA read and the original design strands.

Table 1 summarizes three experiments used to construct these datasets². The experiments varied in parameters such as the number of clusters, strand lengths, cluster size, and the coding scheme used to create the design files, ensuring diversity and robustness for evaluation. Each dataset’s creation included a brute-force mapping of DNA reads to their original strands from the respective design file using edit-distance, which took between 6 and 30 days depending on the sequencing output size. These datasets provide a foundation for evaluating the model’s ability to handle varying levels of complexity and sequencing errors.

Architecture

We propose a deep-learning-based algorithm to compute similarity between raw DNA signals, leveraging the pre-trained layers and weights of the Dorado basecaller [36]. Dorado is an open-source basecaller designed to translate raw electrical signals from Nanopore sequencing into nucleotide sequences. It employs a Conditional Random Field (CRF) architecture that includes convolutional, Long Short-Term Memory (LSTM) [38], and linear layers. The convolutional layers extract salient features, the LSTM layers capture sequential dependencies, and the linear layers align the processed features to the output space. A Clamp layer ensures numerical stability by constraining prediction scores.

To adapt Dorado for clustering tasks, we truncate its architecture after the CRF layer, producing a 1024-dimensional embedding vector. A linear layer with dimensions 1024×500 is appended to map the embeddings to 500 clusters, corresponding to the number of distinct clusters in the training set. This architecture is trained with the ArcFace loss (see Section 3 Loss Function), which enhances the discriminative power of the embeddings by enforcing compact intra-cluster structures and distinct inter-cluster separations.

The model processes raw DNA signals directly as input. Our architecture leverages Dorado’s pre-trained feature extraction capabilities while incorporating clustering-specific components, enabling effective handling of noise and signal variability inherent in DNA data. This design produces robust embeddings suitable for large-scale clustering tasks.

Training Framework. During training, we employed a fine-tuning approach by initializing our model weights with pre-trained weights of the Dorado model and then iteratively updating them during training using the Adam optimizer [18]. The model is trained on the “Microsoft Experiment” dataset, which contains 205,690 samples from 500 selected clusters. The data is split into 70% for training, 15% for validation, and 15% for testing. The performance is measured with a batch

²The “Microsoft Experiment” design file is taken from [35] and the sequenced data is from [33]. The “Deep DNA Test” and “Deep DNA Pilot” design file and sequenced data are from [4].

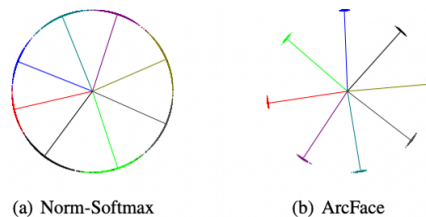


Figure 2: Comparison between Norm-Softmax and ArcFace embeddings. Norm-Softmax projects feature vectors onto a hypersphere but does not enforce explicit angular separation, leading to smaller margins between classes. ArcFace introduces an angular margin, increasing inter-class separability and ensuring compact intra-class clustering [9].

size of 256 on a AMD EPYC7513 server with 1TB RAM and four NVIDIA A6000 GPUs.

Loss Function

Traditional loss functions often struggle with embedding quality in noisy, high-dimensional DNA sequencing datasets. To address this, we implement ArcFace (Additive Angular Margin Loss) [9], which optimizes embedding geometry on a hypersphere by introducing angular margin penalties between same-class embeddings [9, 17].

Let $\mathbf{x}_i \in \mathbb{R}^d$ be the deep feature of the i -th signal sample and $\mathbf{W}_j \in \mathbb{R}^d$ be the j -th column of weight matrix $\mathbf{W} \in \mathbb{R}^{d \times n}$, where embedding dimension $d = 1024$ and number of classes $n = 500$. The cosine similarity between \mathbf{x}_i and \mathbf{W}_j is: $\cos(\theta_j) = \frac{\mathbf{W}_j^T \mathbf{x}_i}{\|\mathbf{W}_j\| \|\mathbf{x}_i\|}$. The ArcFace loss function³ adds margin m to the ground-truth class angle:

$$L = -\frac{1}{N} \sum_{i=1}^N \log \frac{e^{s \cos(\theta_{y_i} + m)}}{e^{s \cos(\theta_{y_i} + m)} + \sum_{j=1, j \neq y_i}^n e^{s \cos(\theta_j)}} \quad (1)$$

where N is batch size and s controls hypersphere radius. This normalization to a hypersphere with optimized angular distances ensures robust cluster separation, making it effective for DNA signal clustering. Figure 2 demonstrates how ArcFace enforces compact intra-cluster embeddings while increasing angular separation between clusters.

4 Evaluation

We examine two aspects of the proposed signal-based approach. First, we analyze our signal embeddings through comparisons with both edit distance-based methods and existing DNA embedding models. Second, we assess the clustering performance of our approach through comprehensive representation and accuracy analyses. We conduct our evaluations on three diverse datasets: *Microsoft Experiment*, *Deep DNA Pilot*, and *Deep DNA Test*. The results demonstrate both the accuracy and computational advantages of our method compared to existing approaches.

From each dataset, we selected subsets containing 50 clusters to ensure a balanced comparison while maintaining computational feasibility. As shown in Table 2, *Deep DNA Pilot* (63,849 samples, large clusters) is our large-scale validation

³ $\cos(\theta_{y_i} + m) = \cos(\theta_{y_i}) \cos(m) - \sin(\theta_{y_i}) \sin(m)$

Dataset	Size	Cluster Size	Use Case
Microsoft Exp.	16,109	Medium	Practical deployment
Deep DNA Test	739	Small	Baseline performance
Deep DNA Pilot	63,849	Large	Large-scale validation

Table 2: Overview of the three datasets created from the experiments.

dataset and presents challenging conditions for data retrieval due to the huge cluster sizes. In contrast, *Deep DNA Test* (739 samples, small clusters) provides a controlled baseline for evaluating performance presents challenges to learn embeddings that distinguish between clusters. Finally, *Microsoft Experiment* (16, 109 samples, medium clusters) strikes a balance in scale and practical deployment considerations. These distinct characteristics ensure a comprehensive assessment of DNA storage clustering methods.

Each dataset provides both DNA signals and their corresponding sequenced reads, enabling direct comparison. To evaluate, we constructed binary similarity matrices for each dataset, where matrix entry $[i, j]$ equals 1 if signals i and j belong to the same cluster, and 0 otherwise. This ground truth serves as the baseline for our quantitative analysis and allows for systematic evaluation of clustering accuracy.

4.1 Performance Analysis of Signal Embeddings

Comparison with edit distance

We evaluate the performance of the *signal-model*'s embedding-based similarity approach against traditional edit-distance methods applied to DNA reads for clustering. The evaluation focuses on both accuracy and computational efficiency.

To assess accuracy, we generated five distance matrices for each dataset: one cosine similarity matrix for the *signal-model* (based on ArcFace loss [9]) and four edit-distance matrices with varying depth constraints. The depth constraint k determines the range of possible edit-distance values $\{0, 1, \dots, k\}$, where k bounds the number of allowed insertions, deletions, or substitutions. We selected k values of 10, 20, 50, and 200, approximately corresponding to 5%, 10%, 25%, and 100% of our experimental DNA storage reads length (see Table 1).

An important distinction between the methods lies in their similarity measures. While edit-distance provides discrete thresholds corresponding to specific numbers of edits, the *signal-model*'s cosine similarity offers continuous values ranging from -1 to 1 , where 1 indicates perfect similarity.

Using these matrices, receiver operating characteristic (ROC) plots were generated. The ROC curve illustrates the trade-off between the true positive (TP) and false positive (FP) values of an ML model. Figure 3 presents ROC curves comparing the *signal-model* against the four baseline models with varying depth (k) values. Models with better performance exhibit ROC curves closer to the top-left corner, indicating a higher TP rate and a lower FP rate. A random model aligns with the diagonal identity line, while the area under the ROC curve (AUC) quantifies performance, normalized to $[0, 1]$, where 1 represents perfect classification.

The results demonstrate that the *signal-model* achieves higher accuracy than the strand-based models across all experiments. For the "Microsoft Experiment", the *signal-model*

attains an AUC of 0.99, significantly outperforming the strand- $k = 200$ (0.81), strand- $k = 50$ (0.80), strand- $k = 20$ (0.57), and strand- $k = 10$ (0.51) models. The sharp turn and linear increase in all curves reflect read pairs exceeding the k -threshold, rendering them equally distant. The strand- $k = 200$ model is the closest in performance to the *signal-model*, as it effectively approximates an unbounded edit-distance calculation over the read length. However, this comes with significantly higher computational complexity.

Similar trends appear for the *Deep DNA Pilot* and *Deep DNA Test* datasets (Figures 3(b) and 3(c)). Notably, the *Microsoft Experiment* achieves better performance because the evaluation clusters share the same data distribution as the training set, although the specific clusters used for evaluation were unseen during training.

Regarding computational efficiency, Figure 4 illustrates the time required for similarity matrix computation across all experiments. The *signal-model* demonstrates remarkable efficiency, requiring **1 to 3 orders of magnitude less time** compared to strand-based approaches. For the strand- $k = xx$ models, computation times increase linearly with k , while the *signal-model* maintains consistent performance regardless of sequence complexity.

Comparison with DNA embedding models

To further validate the *signal-model*'s approach, we compare against open sourced state-of-the-art DNA sequence embedding models: *gena-lm-bert-base* (GLBB), *gena-lm-bert-large-t2t* (GLBL) [11], and *DNABERT* [16]. The GENA-LM models comprise a family of foundational models specifically designed for long DNA sequences, employing transformer-based architectures pre-trained on extensive human DNA sequence data. While the base version (GLBB) uses a standard BERT architecture, the large version (GLBL) incorporates additional transformer layers and attention mechanisms optimized for DNA sequences. DNABERT offers a specialized BERT model adapted for DNA sequences, incorporating k -mer embedding strategies to capture local sequence patterns. It employs a bidirectional encoder architecture specifically tuned for genomic data, with pre-training objectives designed to capture biological sequence properties.

In terms of embedding dimensionality, *DNABERT* and *gena-lm-bert-base* produce 768-dimensional vectors, while *gena-lm-bert-large-t2t* generates 1024-dimensional embeddings matching our *signal-model*'s dimensionality. While these models excel at capturing biologically relevant features in natural DNA sequences, they may not be optimally suited for synthetic DNA storage applications where the sequences don't necessarily follow natural biological patterns.

Figure 5 presents ROC curves comparing these approaches, demonstrating the *signal-model*'s superior performance across all experiments. For the *Microsoft Experiment*, our model achieves an AUC of 0.99, substantially outperforming GLBB (0.64), GLBL (0.70), and *DNABERT* (0.6).

Table 3 provides a unified comparison of both metrics, accuracy (AUC) and computational efficiency (Time), across four models on the three datasets. Our *signal-model* approach significantly outperforms existing DNA models, achieving superior AUC scores (0.92–0.99) compared to (0.6–0.7) for the other DNA-based models. In terms of computational effi-

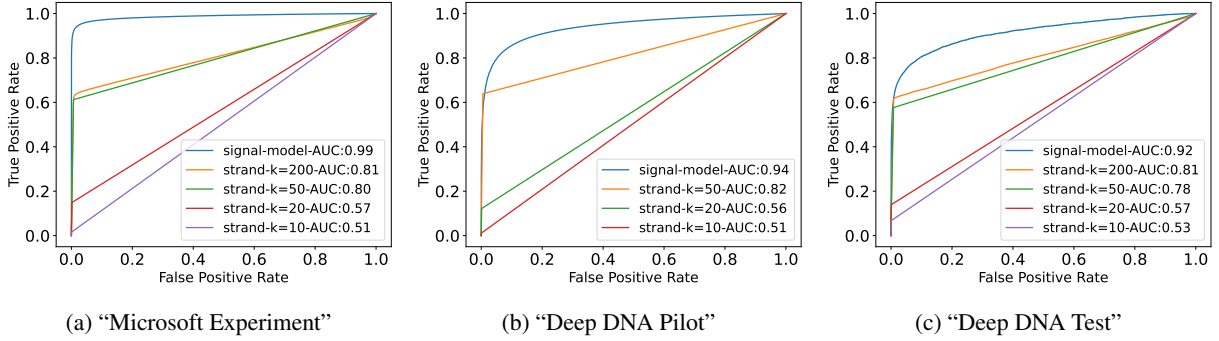


Figure 3: Comparison of DNA signal similarity with *signal-model* embeddings and DNA sequence similarity with edit-distance across datasets.

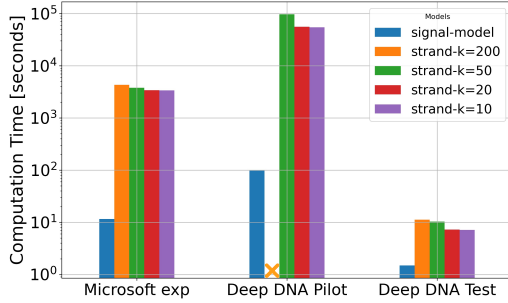


Figure 4: Computation times across three datasets. For the *signal-model*, this includes embedding generation and cosine similarity calculations, while for $\text{strand-}k = xx$ models it covers edit-distance computations. Red crosses mark entries where the runtime exceeded 30 hour.

Dataset	Metric	GLBB	GLBL	DNABERT	<i>signal-model</i>
Microsoft Exp	AUC	0.64	0.70	0.60	0.99
	Time[s]	103.84	173.52	99.25	11.57
Deep DNA Test	AUC	0.64	0.70	0.57	0.92
	Time[s]	1.56	3.53	3.00	1.49
Deep DNA Pilot	AUC	0.60	0.70	0.56	0.94
	Time[s]	156.14	371.91	274.93	98.07

Table 3: Performance comparison of *signal-model* and DNA embedding models across datasets.

ciency, our *signal-model* processes the *Microsoft Exp* dataset in 11.57 seconds compared to 99–173 seconds for other models, demonstrating up to 15x speedup while maintaining higher accuracy.

4.2 Clustering Performance Analysis

To evaluate the *signal-model*’s clustering capabilities, we conduct a systematic analysis across two key dimensions: representation quality and accuracy metrics. Our evaluation employs hierarchical clustering [26] with cosine similarity on the three datasets, comparing against widely adopted DNA data storage clustering algorithms: Clover [28] and Microsoft’s alg [30] (which we independently implemented following their paper’s description), using their suggested parameters. Beyond demonstrating better clustering performance, our *signal-model*

approach eliminates the need for the time-consuming base-calling phase (saving days of computation), while achieving better results compared to DNA-based clustering algorithms. This shows that classical clustering techniques, when applied to our signal-based embeddings, can effectively outperform DNA storage clustering methods.

Representation Learning

Figure 6 provides t-SNE visualizations across the three datasets, offering insights into cluster separability. The *Microsoft Experiment* (Figure 6(a)) exhibits well-defined cluster boundaries with clear separation in the embedding space, demonstrating the model’s ability to effectively distinguish between different clusters under typical conditions. The *Deep DNA Test* results (Figure 6(b)), despite its sparse data distribution, the visualization demonstrates clear cluster separation, with distinct groupings spread across the embedding space. Additionally, the *Deep DNA Pilot* (Figure 6(c)) shows denser cluster formations, reflecting the increased complexity and challenging conditions inherent in larger-scale data. These visualizations across different experimental conditions demonstrate the robustness of our *signal-model*’s approach in capturing meaningful features within DNA signal data.

Clustering Accuracy for DNA

For evaluating clustering performance in DNA storage applications, traditional clustering metrics are insufficient as they do not account for the unique characteristics of DNA storage. We adopt and extend the accuracy measure introduced by [30], specifically designed for DNA storage data retrieval tasks. Let C represent the ground truth clustering and \tilde{C} denote the predicted clustering output from an algorithm. We define the clustering accuracy $\mathcal{A}_{\gamma, \beta}$ with two key parameters: γ controlling the minimum required overlap for correct cluster identification, and β establishing the maximum allowed fraction of false positives. Formally:

Definition 1 (DNA Storage Clustering Accuracy). *For clusters C, \tilde{C} , with parameters $0.5 < \gamma \leq 1$, $0 \leq \beta < 0.5$, and a minimum overlap threshold N , the accuracy of \tilde{C} with respect*

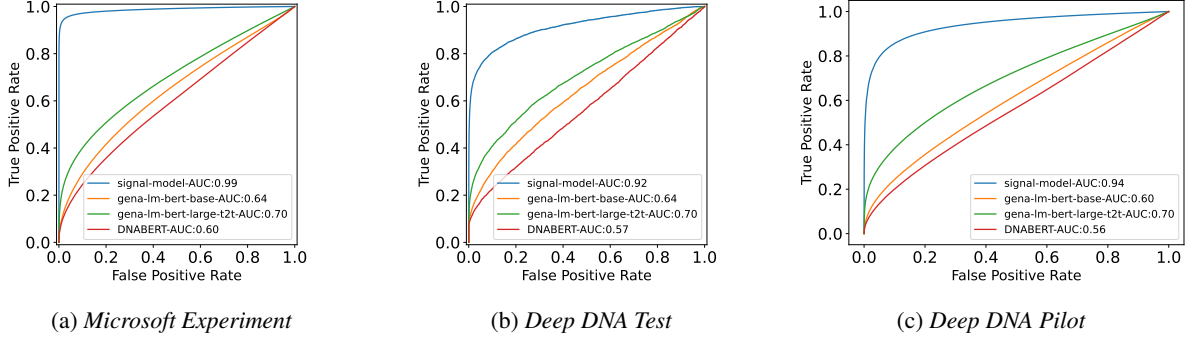


Figure 5: Comparison of DNA signal similarity with *signal-model* embeddings and DNA sequence similarity using DNA embedding models across datasets.

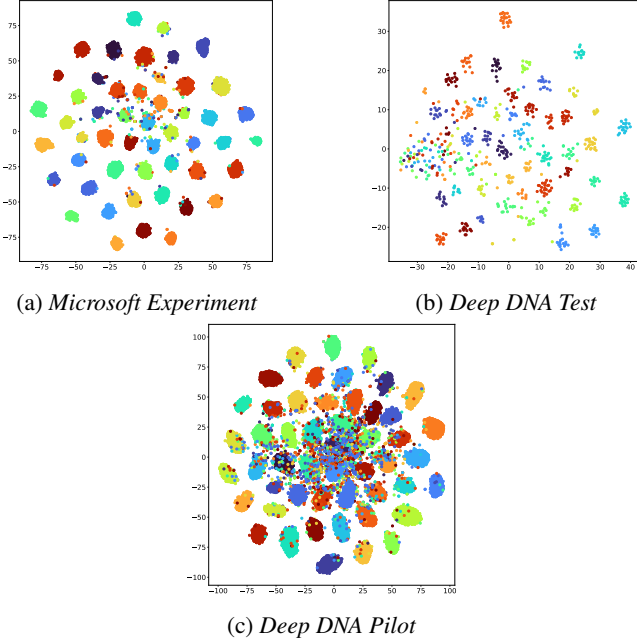


Figure 6: t-SNE analysis of the 50 clusters of each dataset.

to C is:

$$\mathcal{A}_{\gamma,\beta}(C, \tilde{C}) = \max_{\pi} \frac{1}{|C|} \sum_{i=1}^{|C|} \mathbf{1}\{|\tilde{C}_{\pi(i)} \setminus |\tilde{C}_{\pi(i)} \cap C_i| \leq \beta|\tilde{C}_{\pi(i)}| \text{ and } |\tilde{C}_{\pi(i)} \cap C_i| \geq \min(N, \gamma|C_i|)\} \quad (2)$$

where π is a mapping from $\{1, 2, \dots, |C|\}$ to $\{1, 2, \dots, \max(|C|, |\tilde{C}|)\}$.

This definition extends the original formulation in [30] in two significant ways. First, we introduce the parameter β to allow for a controlled fraction of false positives, considering that DNA storage reconstruction algorithms are designed to handle and correct a certain level of errors [33]. Second, we add the constant N to accommodate varying cluster sizes, particularly important for large-scale cluster size. [30]’s accuracy is defined for $\beta = 0$ and under the assumption that the output of sequencing is a small number of noisy DNA reads of each

cluster reference.

The accuracy measure $\mathcal{A}_{\gamma,\beta}$ evaluates clustering quality through two essential conditions. The false positive condition $|\tilde{C}_{\pi(i)} \setminus |\tilde{C}_{\pi(i)} \cap C_i| \leq \beta|\tilde{C}_{\pi(i)}|$ ensures that no more than a β -fraction of elements in each predicted cluster are incorrectly assigned. Additionally, the overlap condition $|\tilde{C}_{\pi(i)} \cap C_i| \geq \min(N, \gamma|C_i|)$ requires either a minimum absolute overlap of N samples or a relative overlap of γ -fraction, whichever is smaller. This interpretation justifies the need for high accuracy and an error fraction: each underlying cluster represents one stored unit of information.

Figure 7 presents accuracy comparisons between our hierarchical clustering algorithm, which leverages *signal-model* embeddings, and Microsoft’s state-of-the-art method for DNA data storage sequences [30]. Clover was excluded from this comparison because it consistently underperformed. Each subplot captures the performance under distinct datasets and parameter variations, illustrating how accuracy changes in response to the false-positive rate $\beta \in \{0, 0.1, 0.2\}$, the overlap determined by the min between the γ threshold, and the constant parameter N . In particular, β governs how much noise is introduced into each cluster (higher β indicates noisier clusters), while $\gamma \in \{0.6, 0.7, 0.8, 0.9, 1.0\}$ in Figures 7 (a) and 7(b), specifying how strictly a produced cluster must overlap with the original ground-truth cluster. In Figure 7 (c), for the large cluster size dataset, we show accuracy as a function of N , since the overlap is effectively determined by $\min(N, \gamma|C_i|)$.

In Figure 7(a), our algorithm consistently achieves higher accuracy than Microsoft’s across all examined noise levels. While both methods experience slight decreases in accuracy under more stringent overlap requirements (larger γ), our algorithm remains comparatively robust, for smaller β values our algorithm achieve 94%, while retaining accuracy above 60% – 70% for larger β , whereas Microsoft’s method frequently hovers below 30%. In Figure 7(b), which corresponds to a smaller dataset, both algorithms show reduced performance due to tighter constraints on β and γ . Nonetheless, our method still outperforms Microsoft’s: for $\beta = 0.2$, we achieve 50% accuracy versus Microsoft’s 30%. For both plots, N is set to 200, as it is enough for reconstruction purposes and does not affect the overlap fraction.

Finally, Figure 7(c) presents the results for the large dataset,

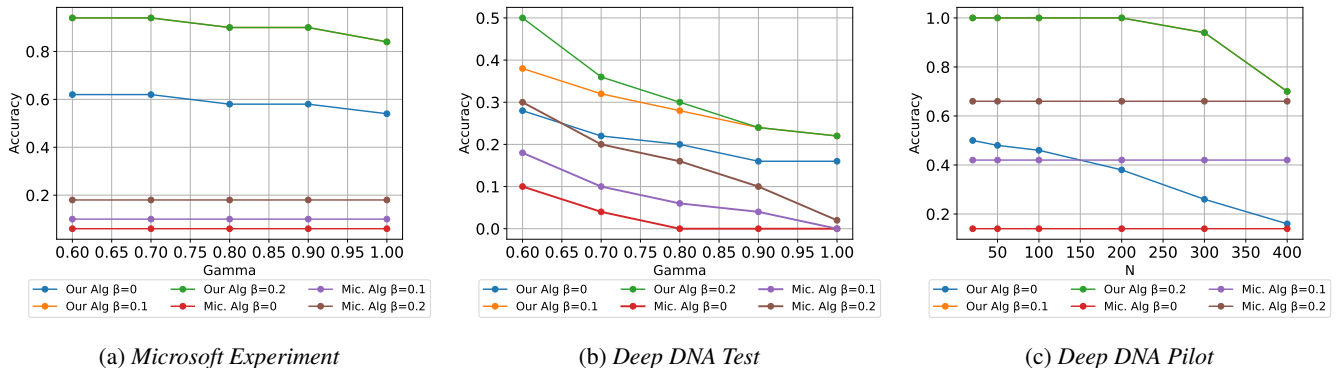


Figure 7: Comparison to Microsoft algorithm. Figures (a) and (b) plot $\mathcal{A}_{\gamma,\beta}$ for varying $\gamma \in \{0.6, 0.7, 0.8, 0.9, 1.0\}$ and $N = 200$. (c) plots $\mathcal{A}_{\gamma,\beta}$ for varying $N \in \{20, 50, 100, 200, 400\}$ due to *Deep DNA Pilot* huge clusters that in this case $N = \min(N, \gamma|C_i|)$. All figures include plots for $\beta \in \{0, 0.1, 0.2\}$ as the false positive rate in the clusters. In (a) and (c) our Alg $\beta = 0.1$, our Alg $\beta = 0.2$ have the same accuracy.

Dataset	Alg	Recall	Precision	F1	No. Clusters
Microsoft exp	<i>signal-model</i>	0.794	0.994	0.883	145
	clover	0.13	0.042	0.064	40
	Mic.	0.688	0.171	0.274	26
Deep DNA Test	<i>signal-model</i>	0.650	0.563	0.604	45
	clover	0.212	0.024	0.044	33
	Mic.	0.56	0.598	0.578	75
Deep DNA Pilot	<i>signal-model</i>	0.357	0.953	0.519	387
	clover	0.39	0.101	0.161	44
	Mic.	0.577	0.668	0.619	2090

Table 4: Comparison of clustering algorithms across datasets.

where the effect of γ diminishes because N is effectively bounded by $\min(N, \gamma|C_i|)$. Our algorithm achieves perfect accuracy at moderate N values and remains resilient even as N increases to 400. By contrast, Microsoft’s approach yields a vast majority of clusters of size 1 and merges many sequences into a few large clusters, resulting in stable but substantially lower accuracy overall. In fact, it creates 90% of its clusters with size 1 and 97% with sizes below 19, which are redundant given the dataset’s average cluster size of 1,300. Moreover, in the few large clusters it does form, it often merges distinct groups, adversely affecting the β fraction and explaining the 20% accuracy boost observed at $\beta = 0.2$. Nevertheless, that boost is overshadowed by the balanced cluster-size distribution our method maintains, as evidenced by its perfect accuracy for $\beta = 0.1$. Overall, these findings confirm that our hierarchical signal-model algorithm outperforms the existing state-of-the-art across various noise levels, overlap thresholds, and dataset sizes, underscoring its suitability for a successful reconstruction of DNA data storage tasks.

Clustering Robustness

Table 4 presents an evaluation of our algorithm against standard clustering metrics across all datasets. The performance is measured using three key metrics: Recall ($\frac{TP}{TP+FN}$), which indicates the model’s ability to identify all positive samples; Precision ($\frac{TP}{TP+FP}$), which measures the model’s accuracy in positive predictions; and F1 score, the harmonic mean of precision and recall that provides a balanced assessment of the

model’s overall performance.

The results demonstrate consistent strong performance across different experimental conditions. On the *Microsoft Experiment* dataset, our algorithm achieves superior performance across all metrics. For the *Deep DNA Test* dataset, while our and Microsoft algorithms show comparable performance, our approach maintains an edge in both Recall and F1 scores. Even on the challenging *Deep DNA Pilot* dataset, which features exceptionally large clusters, our algorithm achieves a competitive F1 score of 0.519 compared to Microsoft’s 0.619. Notably, while our and Microsoft algorithms process the complete dataset, Clover’s approach discards a significant portion of the input reads—retaining only 3% (486 of 16,109) reads in the *Microsoft Experiment* and less than 1% (476 of 63,849) in the *Deep DNA Pilot*. We achieve similar results with Microsoft alg for Rand-Index (0.98), Homogeneity (± 0.8), Completeness (± 0.8) and V-measure (± 0.8) scores, while Clover does not.

5 Conclusion

This work demonstrates the transformative potential of directly utilizing raw DNA signals in the analysis of Nanopore sequencing data, particularly for DNA storage applications. By leveraging a signal-based approach, our method achieves significant improvements in computational efficiency while maintaining high clustering accuracy. Our experimental results demonstrate the effectiveness of the signal-model’s embeddings across multiple datasets, showing robust performance in generating discriminative representations that enable efficient clustering.

These findings underscore the importance of preserving raw signal information, often discarded during basecalling, for downstream DNA data storage tasks. Directly clustering raw signals may further reduce the risk of losing critical details essential for accurate data reconstruction. Future research could extend the signal-model to other sequencing applications—such as RNA—and investigate more advanced neural architectures for enhanced robustness. Moreover, specialized clustering algorithms and improved scalability techniques could unlock the full potential of this signal-based paradigm in DNA storage and beyond.

References

- [1] Leon Anavy, Inbal Vaknin, Orna Atar, Roei Amit, and Zohar Yakhini. Data storage in DNA with fewer synthesis cycles using composite DNA letters. *Nature biotechnology*, 37(10):1229–1236, 2019.
- [2] Philipp L Antkowiak, Jory Lietard, Mohammad Zalbagi Darestani, Mark M Somoza, Wendelin J Stark, Reinhard Heckel, and Robert N Grass. Low cost DNA data storage using photolithographic synthesis and advanced information reconstruction and error correction. *Nature communications*, 11(1):5345, 2020.
- [3] Ergude Bao, Tao Jiang, Isgouhi Kaloshian, and Thomas Girke. Seed: efficient clustering of next-generation sequences. *Bioinformatics*, 27(18):2502–2509, 2011.
- [4] Daniella Bar-Lev, Itai Orr, Omer Sabary, Tuvi Etzion, and Eitan Yaakobi. Deep DNA storage: Scalable and robust DNA storage via coding theory and deep learning. *arXiv preprint arXiv:2109.00031*, 2021.
- [5] Dvir Ben Shabat, Adar Hadad, Avital Boruchovsky, and Eitan Yaakobi. Gradhc: Highly reliable gradual hash-based clustering for DNA storage systems. *bioRxiv*, pages 2023–10, 2023.
- [6] James Bornholt, Randolph Lopez, Douglas M Carmean, Luis Ceze, Georg Seelig, and Karin Strauss. A dna-based archival storage system. In *Proceedings of the twenty-first international conference on architectural support for programming languages and operating systems*, pages 637–649, 2016.
- [7] Douglas Carmean, Luis Ceze, Georg Seelig, Kendall Stewart, Karin Strauss, and Max Willsey. Dna data storage and hybrid molecular–electronic computing. *Proceedings of the IEEE*, 107(1):63–72, 2018.
- [8] Shubham Chandak, Joachim Neu, Kedar Tatwawadi, Jay Mardia, Billy Lau, Matthew Kubit, Reyna Hulett, Peter Griffin, Mary Wootters, Tsachy Weissman, et al. Overcoming high nanopore basecaller error rates for DNA storage via basecaller-decoder integration and convolutional codes. In *ICASSP 2020-2020 IEEE International Conference on Acoustics, Speech and Signal Processing (ICASSP)*, pages 8822–8826. IEEE, 2020.
- [9] Jiankang Deng, Jia Guo, Niannan Xue, and Stefanos Zafeiriou. Arcface: Additive angular margin loss for deep face recognition. In *Proceedings of the IEEE/CVF conference on computer vision and pattern recognition*, pages 4690–4699, 2019.
- [10] Yaniv Erlich and Dina Zielinski. Dna fountain enables a robust and efficient storage architecture. *Science*, 355(6328):950–954, 2017.
- [11] Veniamin Fishman, Yuri Kuratov, Aleksei Shmelev, Maxim Petrov, Dmitry Penzar, Denis Shepelin, Nikolay Chekanov, Olga Kardymon, and Mikhail Burtsev. Gena-lm: a family of open-source foundational dna language models for long sequences. *bioRxiv*, pages 2023–06, 2023.
- [12] Limin Fu, Beifang Niu, Zhengwei Zhu, Sitao Wu, and Weizhong Li. Cd-hit: accelerated for clustering the next-generation sequencing data. *Bioinformatics*, 28(23):3150–3152, 2012.
- [13] Nick Goldman, Paul Bertone, Siyuan Chen, Christophe Dessimoz, Emily M LeProust, Botond Sipos, and Ewan Birney. Towards practical, high-capacity, low-maintenance information storage in synthesized dna. *nature*, 494(7435):77–80, 2013.
- [14] Dan Gusfield. Algorithms on strings, trees, and sequences: Computer science and computational biology. *Acm Sigact News*, 28(4):41–60, 1997.
- [15] Miten Jain, Hugh E Olsen, Benedict Paten, and Mark Akeson. The oxford nanopore minion: delivery of nanopore sequencing to the genomics community. *Genome biology*, 17:1–11, 2016.
- [16] Yanrong Ji, Zhihan Zhou, Han Liu, and Ramana V Davuluri. Dnabert: pre-trained bidirectional encoder representations from transformers model for dna-language in genome. *Bioinformatics*, 37(15):2112–2120, 2021.
- [17] Zafran Khan, Abhijeet Boragule, Brian J d’Auriol, and Moongu Jeon. Improvised contrastive loss for improved face recognition in open-set nature. *Pattern Recognition Letters*, 180:120–126, 2024.
- [18] Diederik P Kingma and Jimmy Ba. Adam: A method for stochastic optimization. *arXiv preprint arXiv:1412.6980*, 2014.
- [19] Neal Koblitz, Alfred Menezes, and Scott Vanstone. The state of elliptic curve cryptography. *Designs, codes and cryptography*, 19:173–193, 2000.
- [20] Nobuaki Kono and Kazuharu Arakawa. Nanopore sequencing: Review of potential applications in functional genomics. *Development, growth & differentiation*, 61(5):316–326, 2019.
- [21] Gad M Landau and Uzi Vishkin. Fast parallel and serial approximate string matching. *Journal of algorithms*, 10(2):157–169, 1989.
- [22] Emily M LeProust, Bill J Peck, Konstantin Spirin, Heather Brummel McCuen, Bridget Moore, Eugeni Namsaraev, and Marvin H Caruthers. Synthesis of high-quality libraries of long (150mer) oligonucleotides by a novel depurination controlled process. *Nucleic acids research*, 38(8):2522–2540, 2010.
- [23] Hong-Liang Li, Yi-He Pang, and Bin Liu. Bioseq-blmm: a platform for analyzing dna, rna and protein sequences based on biological language models. *Nucleic acids research*, 49(22):e129–e129, 2021.
- [24] Wei Mao, Suhas N Diggavi, and Sreeram Kannan. Models and information-theoretic bounds for nanopore sequencing. *IEEE Transactions on Information Theory*, 64(4):3216–3236, 2018.
- [25] Brendon McBain and Emanuele Viterbo. An information-theoretic approach to nanopore sequencing for DNA storage. *IEEE BITS the Information Theory Magazine*, pages 1–13, 2024.

- [26] Fionn Murtagh and Pedro Contreras. Algorithms for hierarchical clustering: an overview. *Wiley Interdisciplinary Reviews: Data Mining and Knowledge Discovery*, 2(1):86–97, 2012.
- [27] Lee Organick, Siena Dumas Ang, Yuan-Jyue Chen, Randolph Lopez, Sergey Yekhanin, Konstantin Makarychev, Miklos Z Racz, Govinda Kamath, Parikshit Gopalan, Bichlien Nguyen, et al. Random access in large-scale DNA data storage. *Nature biotechnology*, 36(3):242–248, 2018.
- [28] Guanjin Qu, Zihui Yan, and Huaming Wu. Clover: tree structure-based efficient DNA clustering for DNA-based data storage. *Briefings in Bioinformatics*, 23(5):bbac336, 2022.
- [29] Thanawin Rakthanmanon, Bilson Campana, Abdullah Mueen, Gustavo Batista, Brandon Westover, Qiang Zhu, Jesin Zakaria, and Eamonn Keogh. Searching and mining trillions of time series subsequences under dynamic time warping. In *Proceedings of the 18th ACM SIGKDD international conference on Knowledge discovery and data mining*, pages 262–270, 2012.
- [30] Cyrus Rashtchian, Konstantin Makarychev, Miklos Racz, Siena Ang, Djordje Jevdjic, Sergey Yekhanin, Luis Ceze, and Karin Strauss. Clustering billions of reads for DNA data storage. *Advances in Neural Information Processing Systems*, 30, 2017.
- [31] Eric Sven Ristad and Peter N Yianilos. Learning string-edit distance. *IEEE Transactions on Pattern Analysis and Machine Intelligence*, 20(5):522–532, 1998.
- [32] John Rydning. Worldwide IDC global datasphere forecast, 2022–2026: Enterprise organizations driving most of the data growth. Technical report, Technical Report, 2022.
- [33] Omer Sabary, Alexander Yucovich, Guy Shapira, and Eitan Yaakobi. Reconstruction algorithms for DNA-storage systems. *Scientific Reports*, 14(1):1951, 2024.
- [34] Pavel Senin. Dynamic time warping algorithm review. *Information and Computer Science Department University of Hawaii at Manoa Honolulu, USA*, 855(1-23):40, 2008.
- [35] Sundara Rajan Srinivasavaradhan, Sivakanth Gopi, Henry D Pfister, and Sergey Yekhanin. Trellis bma: Coded trace reconstruction on ids channels for DNA storage. In *2021 IEEE International Symposium on Information Theory (ISIT)*, pages 2453–2458. IEEE, 2021.
- [36] Nanopore Technologies. Dorado: A neural network model for nanopore sequencing. <https://github.com/nanoporetech/dorado>, 2024. Accessed: 2024-05-19.
- [37] SM Hossein Tabatabaei Yazdi, Ryan Gabrys, and Olga Milenkovic. Portable and error-free DNA-based data storage. *Scientific reports*, 7(1):5011, 2017.
- [38] Yong Yu, Xiaosheng Si, Changhua Hu, and Jianxun Zhang. A review of recurrent neural networks: Lstm cells and network architectures. *Neural computation*, 31(7):1235–1270, 2019.
- [39] Eduard Zorita, Pol Cusco, and Guillaume J Filion. Starcode: sequence clustering based on all-pairs search. *Bioinformatics*, 31(12):1913–1919, 2015.